Applied Catalysis B: Environmental 140–141 (2013) 348–355

Contents lists available at SciVerse ScienceDirect

Applied Catalysis B: Environmental

journal homepage: www.elsevier.com/locate/apcatb

Photocatalytic degradation of Remazol Brilliant Blue® by sol–gel derived carbon-doped TiO_2

Michael J. Mattle [1], K. Ravindranathan Thampi *

Laboratory of Photonics and Interfaces, ISIC, École Polytechnique Fédérale de Lausanne (EFPL), CH-1015, Lausanne, Switzerland

ARTICLE INFO

Article history:
Received 7 December 2012
Received in revised form 16 March 2013
Accepted 2 April 2013
Available online 17 April 2013

Keywords:
Carbon-doped TiO_2
Sol–gel method
Photocatalytic oxidation
Remazol Brilliant Blue®
Full and cut-off sunlight

ABSTRACT

A simple, cheap and reproducible method to produce a C-doped TiO_2 photocatalyst is presented, which can harvest visible light. This doped catalyst is able to degrade a stable organic dye molecule, Remazol Brilliant Blue® (RBB), under sunlight and visible light alone and its activity is compared to P25. XPS analysis clearly showed that carbon was introduced into the TiO_2 lattice but at much lower doping levels than initially added during the synthesis. BET and diffuse reflectance spectroscopy indicated that the doped catalysts had larger surface area and improved light absorption in the visible region than P25. However, under full sunlight this did not translate into improved photocatalytic activity when compared to P25. Even though the UV cut-off sunlight spectrum permitted P25 to discolor RBB, no actual dye mineralization was observed by total organic carbon (TOC) analysis. In contrast, the doped catalyst did not only achieve discoloration of RBB but also removed 70% of organic carbon. This gives the doped catalyst a clear advantage to operate with visible light alone, which can be produced in a much more economical way, and may therefore reduce treatment costs of wastewater from textile and other industries using dyes. Among several reactive dyes, RBB was particularly found to be the most recalcitrant to discoloration with TiO_2 and this study opens a way to address this issue. The photocatalytic mechanism is discussed.

1. Introduction

Semiconductor based photocatalysis has been identified as an effective method to alleviate very low concentrations of pollutants in air and water [1,2]. Among several suitable semiconductor materials, TiO_2 has been accepted as the most widely studied and used photocatalytic material, due to its strong catalytic activity, its low cost, and photo-stability [3,4]. However, the widespread practical use of TiO_2 as a photocatalyst has been hampered by its large band gap (3.2 eV for anatase TiO_2), which requires ultraviolet radiation ($\lambda < 380$ nm, only 5% of the terrestrial solar spectrum) for photocatalytic activation. The cost of producing UV light using lamps is expensive, therefore, it is desirable to develop photocatalysts that are active upon visible light excitation, such that the solar spectrum or even domestic lighting systems could be used for photoactivation [5].

The modification of TiO_2 itself for absorbing visible light, without losing TiO_2's overall photocatalytic activity (UV + visible light), has become one of the actively researched topics today in the field of photocatalysis [6–9]. One approach is to use metal ions of Fe, Cr, Ni, etc., for substituting Ti^{4+} in TiO_2 [10–12], and another route is to form Ti^{3+} sites, by introducing oxygen vacancies, in TiO_2 lattices [13,14].

The chemical doping of metal ions into TiO_2, to achieve visible light absorption, was performed in the past [15,16]. However, these doped systems are thermally unstable [16] and in many such systems, the doped metal ions existed only as impurities, which enhanced the rate of recombination of the photo-produced electrons and holes [17]. Anpo [18] worked with an advanced high-voltage metal-ion implantation method, which dramatically modified the electronic properties of TiO_2.

Recently, doping TiO_2 with non-metal atoms has also received a lot of attention [19–26]. For example, Asahi et al. [19], Khan et al. [20], and Sakthivel and Kisch [21], have reported that doping TiO_2 with nitrogen or carbon could also sufficiently shift its optical response from UV to more visible wavelengths.

Metal doping can be achieved easily by physical methods, whereas carbon and nitrogen doping are done by severe chemical methods. In general, solution based methods are less capital intensive at manufacturing scale. Therefore, we report here a simple solution based method to produce high surface area carbon-modified TiO_2 catalyst, using melamine borate as a complexing agent with titanium tetrachloride as a precursor for TiO_2. This catalyst was then used to study the degradation of a synthetic dye. Dyes

* Corresponding author. Present address: School of Chemical and Bioprocess Engineering, University College Dublin, Belfield, Dublin 4, Ireland.
E-mail address: ravindranathan.thampi@ucd.ie (K.R. Thampi).
[1] Present address: Laboratory of Environmental Chemistry, School of Architecture, Civil and Environmental Engineering (ENAC), École Polytechnique Fédérale de Lausanne (EPFL), CH-1015, Lausanne, Switzerland.

0926-3373/$ – see front matter © 2013 Elsevier B.V. All rights reserved.
http://dx.doi.org/10.1016/j.apcatb.2013.04.020

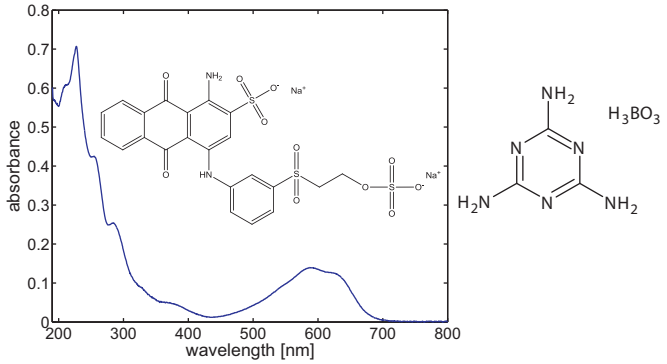

Fig. 1. UV–vis absorbance spectrum of RBB (5 ppm/L) and its chemical structure (left), structure of melamine borate (right).

are extensively used in textile and printing industries and about 30% of synthetic reactive dyes consumed in textile processes are lost due to chemical modifications during the dyeing process [27]. Remazol Brilliant Blue® (RBB, see Fig. 1) was chosen in this study as it has been detected (>40 ppm) in effluents of textile industries in Southern Europe [28]. As it is not biodegradable, it may remain in the environment for a long period of time (its half-life was estimated around 46 years [29]). Additionally, RBB was evaluated to be toxic by microtox assay at very low concentrations (30 ppm) [30].

Among several reactive dyes, RBB was particularly found to be the most recalcitrant to discoloration with TiO_2 under UV_{254} [31]. Further, the removal by TiO_2 photocatalysis was evaluated less economical compared to other methods due to the high cost of artificial UV light [32]. Hence, to render photocatalysis an interesting option, we decided to test the performance of a C-doped catalyst, which harvests visible light, to degrade this stable dye. The results were compared to Degussa P25 TiO_2, which has become a benchmark for comparing the photocatalytic activity of different photocatalysts, due to its high activity [33–36]. The catalysts were tested under simulated sunlight with and without a cut-off filter blocking wavelengths <400 nm.

2. Material and methods

2.1. Preparation of C-doped TiO_2

The detailed synthesis is described elsewhere [37]. In brief: melamine borate (3.4 g, for structure see Fig. 1) was dissolved in 0.5 L de-ionized water and filtered (589[1] Black ribbon ashless from Schwarzband) after 1.5 days of stirring at room temperature. In parallel, 14 mL of $TiCl_4$ (≥99.0% (AT), Fluka) was dissolved dropwise in 1.9 L distilled water cooled at 2–4 °C. To 360 mL of this solution, various aliquots of the aqueous melamine borate solution were added (e.g. 28 mL corresponded to 4 carbon in mol%). Further, 4 M NH_4OH (Riedel-de Haen, Germany) was added dropwise until pH 5 was reached and a white precipitate appeared. The suspension was kept overnight under stirring before filtering and washing repeatedly with warm deionized water to eliminate the remaining chloride (tested by Ag^+). The precipitate was dried overnight at around 125 °C and then heated at 400 °C, for 1 h (heating rate: 600 °C/h). The catalysts were yellow in color when doped with melanime borate, however white otherwise. The material was used for further experiments after manual grinding with an agate mortar and a pestle.

2.2. Catalyst characterization

Diffuse Reflectance Spectra (DRS) were recorded using a Varian Cary 5 UV–Vis–NIR spectroscope fitted with an 11 cm diameter integrating sphere coated with polytetrafluoroethylene (PTFE) [38]. First, the catalyst powders (1.5 g) were spread homogenously onto a microscope slide over an area of about 2.5 cm × 2.3 cm and then covered with a second microscope slide to keep the powder intact. The sample was analyzed relative to the standard reflectance of a PTFE coated plate placed at the measurement port, which corresponded to 100% reflectance, whereas the calibration of 0% reflectance was performed when the port was left open.

A Micromeretics ASAP 2010 nitrogen adsorption–desorption apparatus was used to determine BET surface areas. Pore size distributions were calculated using the Barrett–Johner–Halenda (BJH) method.

The X-ray photoelectron spectroscopy (XPS) measurements were done by Axis Ultra instrument (Kratos analytical, Manchester, UK) under ultra-high vacuum conditions (<10^{-8} Torr), using a monochromatic Al Kα X-ray source (1486.6 eV). The source power was maintained at 150 W (10 mA, 15 kV). The emitted photoelectrons were sampled from a square area of 750 μm × 350 μm. Gold (Au $4f_{7/2}$) and copper (Cu $2p_{3/2}$) lines at 84.0 and 932.6 eV, respectively, were used for calibration, and the adventitious carbon 1s peak at 285 eV as an internal standard to compensate for any charging effects. Sputtering of the surface by an ion beam was used to remove pollution. Quantification was done by relative sensitivity factors provided by the supplier.

X-ray diffraction (XRD) patterns were acquired with a Bruker D8 Discover diffractometer in Bragg–Brentano mode, using Cu Kα radiation (1.540598 Å) and a Ni β-filter. Spectra were measured with a linear silicon strip 'Lynx Eye' detector from 2θ = 10–90°. Reflection patterns were matched to the PDF-4+ database (ICDD).

Dynamic light scattering (DLS) was obtained by Zetasizer (Malvern Instruments, Nano ZS). The instrument was run in backscattering mode (173°) at 25 °C and the duration of each measurement was selected automatically by the instrument software. Results were reported as the z-average value in radius, which corresponds to the intensity-weighted mean hydrodynamic radius of the entirety of particles measured. The catalysts (5 mg) were dispersed in 50 mL pre-filtered water (cellulose nitrate membrane filter; 0.1 μm pore size; Whatman GmbH, Dassel, Germany), ultrasonicated and let equilibrated under stirring for one hour before analysis. Each measurement was repeated at least five times and averaged.

2.3. Photochemical experiments

Photomineralization performance of the synthesized catalysts was studied in the aqueous phase by oxidizing RBB (CyStar Textilfarben GmbH & Co., Frankfurt, Germany) under full and cut-off (>400 nm) sunlight. In brief: 50 mg of catalyst powder was suspended in small glass bottles containing 50 mL of 10 ppm (in carbon content) of RBB. Before illumination the suspensions were purged with oxygen for 10 min, in dark and under stirring.

The irradiation source was a solar simulator (100 mW cm^{-2}, SUNTEST CPS plus, ATLAS), where the samples were kept at 40 °C, under constant stirring (700 rpm). For photocatalytic experiments using only visible light, appropriate 400 nm cut-off filters were employed.

The degradation of the organic dye was studied by removing 5 mL of the suspension, which was immediately filtered (Durapore® membrane filter (0.45 μm, 13 mm diameter) from Millipore), at different time intervals. The UV absorption peak at 232 nm of RBB (Fig. 1) was used to determine the initial compound remaining in the sample (8452A Diode array spectrophotometer, Hewlett Packard). The Total Organic Carbon (Shimadzu TOC-V_{SCN} analyzer, samples were purged before injection) was analyzed to measure the total mineralization that occurred as a result of the photocatalytic reaction. All catalytic experiments were at least performed in

duplicates. A linear regression fitted to the initial rate showed a 95% confidence level for the fit.

3. Results and discussion

The physical properties of the synthesized materials were characterized using XPS, XRD, diffuse reflectance spectroscopy (DRS), BET surface area, porosimetry and dynamic light scattering (DLS).

In a parallel study [37], elemental analyses have showed that only very little carbon was included in the lattice of the doped catalysts (0.003–0.005 mol% instead of 1–4% nominal doping as intended). It is therefore wrong to assume that the 4% carbon doped catalyst contained 4% carbon. However, in order to avoid confusion, we always named catalysts according to the nominal amount of carbon added during the catalyst production.

3.1. XPS and XRD results

The XPS analysis was performed to confirm the incorporation of carbon atoms into the TiO_2 lattice, whereas XRD spectra were recorded to determine the crystal structure of the doped catalysts. The C 1s core levels in the XPS spectra revealed peaks at 286.2 eV and 288.7 eV, apart from the adventitious elemental carbon at 284.8 eV. As discussed elsewhere [37], the two former peaks could not be attributed to carbon doping but were interpreted as adsorbed carbon species on the surface of the catalysts. The catalysts were then sputtered with argon ions to remove the outer layer of the catalysts and an additional peak 282.1 appeared (1.5 mol%), indicating that carbon was substitutionally doped in place of oxygen in the TiO_2 lattice [39–42], while the other peaks disappeared with increasing sputtering.

For the doped catalysts, the binding energies increased by 0.1–0.5 (at 458.3 eV) for Ti $2p_{3/2}$ and by 0.2–0.6 (at 529.6 eV) for O 1s compared to the blank catalyst. These shifts may indicate lattice distortion due to doping. However, no such increase was observed for the catalyst doped with 20% carbon, indicating that even though more carbon was present during the synthesis it was probably not incorporated into the TiO_2 structure.

The XRD peaks for all carbon doped catalysts showed anatase phase peaks. An additional minor peak around 31° appeared for catalysts doped with at least 4% carbon, indicating that a larger content of melamine borate present during the production process hindered a total transformation into anatase phase but that a small proportion of brookite was formed, too (data not shown).

It is important to note here that neither nitrogen nor boron doping occurred in spite of the fact that melamine borate was the doping source [37].

3.2. Reflectance spectra

Reflectance spectroscopy revealed that all doped catalysts irrespective of doping concentration showed similar light absorption spectra. Only the 20% doped sample showed a slightly stronger absorption in the UV range than the other doped catalysts (Fig. 2). The elemental analysis indicated that doping with 1–4% carbon did not influence the carbon present in the final catalyst [37], therefore, a change in light absorption was not expected, either. Unlike P25, the doped catalysts started to absorb light from 500 nm downwards. Even the blank sample showed a small absorption below 500 nm, however clearly less pronounced than for the doped samples.

All C-doped TiO_2 and the blank sample to a much smaller extent showed absorption in the wavelength range >500 nm when compared to P25. This red shift is either due to localized states slightly above the valence band or due to the introduction of color centers [43,44]. The XPS data showed that a small amount of carbon was present within the TiO_2 lattice, which probably produced localized states but was too low to produce a band gap narrowing [45]. The fact that the blank catalyst also absorbed some visible light suggests that color centers due to oxygen vacancies developed on the surface of the oxide during the heating process. The highest doping concentration (20%) showed an important increase in the visible light absorption, which could be due to carbonaceous species on the catalyst's surface [46] or a modification in the crystal structure [19].

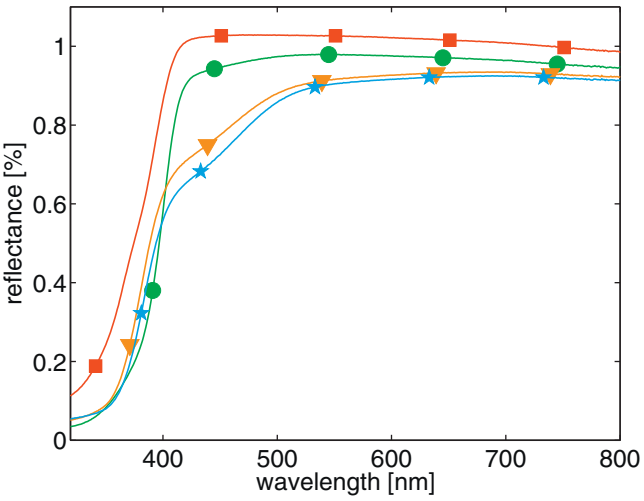

Fig. 2. Reflectance spectra of blank (●), 4% (▼) and 20% (★) C-doped TiO_2 in comparison with the spectra for P25 sample (■).

Around 400 nm, for all TiO_2 samples, including P25, the reflectance values decreased fairly quickly, as expected for TiO_2. The most important part of the spectrum, useful for visible light induced photocatalysis, however, is above 400 nm. The doped catalysts showed increased absorption in this range compared to P25, which may allow them to be photocatalytically active even under visible light only.

3.3. BET surface area and average particle size

The BET surface area of the carbon doped TiO_2 catalysts prepared in this study were between 130 and 150 m^2/g (see Table 1), which is more than double the surface area of commercial P25 (58 m^2/g). The undoped catalyst (blank) showed a relatively smaller surface area (119 m^2/g), indicating that the carbon doping increased the catalyst's surface area. However, the increase of carbon added during the synthesis had little influence on the observed surface area, as the catalysts (1–4%) showed only slightly larger surface areas and pore diameters than the ones doped with more carbon (8–20%).

A very narrow pore size distribution, which centered around 6–12 nm, in pore diameter, was observed for the carbon doped catalysts compared to the un-doped TiO_2 prepared by the same route (see Fig. 3). The latter sample had wider a distribution of

Table 1
BET surface area, average pore radius and average particle size.

TiO_2 catalyst	BET surface area (m^2/g)	Average pore radius (nm)	Particle radius in solution (nm, measured by DLS)
P25	53.6	7.1	150 ± 10
Blank	118.7	8.6	180 ± 10
1%	141.1	4.8	570 ± 80
2%	149.2	4.9	230 ± 20
4%	148.2	5.5	490 ± 40
8%	132.2	3.3	320 ± 60
12%	131.5	3.3	350 ± 130
20%	134.6	3.0	500 ± 110

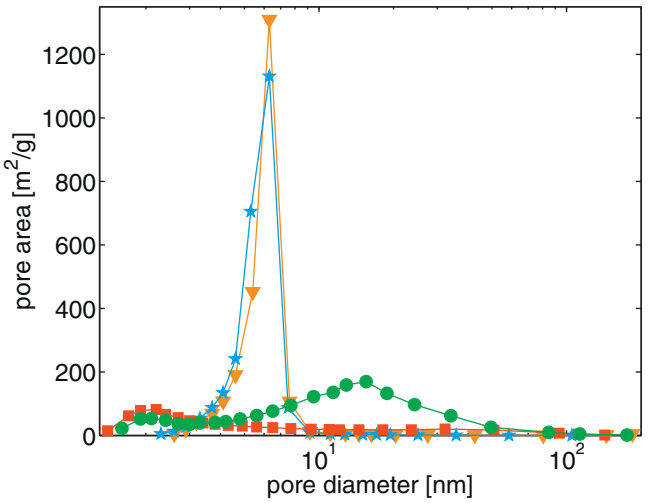

Fig. 3. Pore area versus pore diameter for the different catalysts: 8% doped catalyst (▼), 20% doped catalyst (★), blank catalyst (●) and P25 (■).

pore diameters in the range of 1.5–40 nm, with a peak around 16 nm. Similarly, P25 exhibited a wider distribution of pore sizes, however, the maximum was very low at around 2 nm. Hence, the doping produced a catalyst more homogeneous in terms of pore size distribution compared to the undoped catalysts.

3.4. Dynamic light scattering (DLS)

The particle size determination from XRD data using the Scherrer equation [47] for the peak at $2\theta = 25.6^{\circ}$ (with shape factor 0.94) revealed that the size range was between 6.2 and 8.4 nm for the doped particles, whereas for P25 the size was slightly larger (14 nm). In contrast, the DLS measurements (shown in Table 1) showed hydrodynamic radii ranging between 150 and 570 nm. P25 seemed to aggregate the least with a hydrodynamic radius of around 150 nm, followed by the blank catalyst (180 nm). The doped catalysts were slightly larger varying between 230 and 570 nm, but no pattern between carbon doping level and hydrodynamic diameter could be established. The variability of sizes observed for the doped catalysts may originate from the manual grinding.

Larger aggregates were observed to have higher photocatalytic efficiencies [48]. Therefore, doped catalyst could be more efficient due to their larger aggregate sizes in addition to their ability to absorb longer wavelengths and their increased BET surface areas. It should be noted that in the doped samples a limited number of larger particles were also present, which could not be analyzed by DLS, as they settled during measurements.

3.5. Photocatalysis – degradation of Remazol Brilliant Blue® (RBB)

Two types of experiments were performed to evaluate how efficiently the C-doped visible light active catalysts could degrade RBB compared to commercial P25. Firstly, the experiments were run under simulated full sunlight irradiation, and secondly, under simulated sunlight with 400 nm cut-off filters. The second series of experiments were performed to test the ability of the C-doped catalyst to operate under visible sunlight only, which is much cheaper to generate than UV light. The UV absorption peak at 232 nm (Fig. 1) was chosen to determine the amount of original dye remaining in solution. Further, TOC analysis was performed to estimate the level of total mineralization of RBB.

Initially, P25 was employed to determine the optimum pH level for RBB degradation (neutral pH ± 0.8/1.5). Even though P25

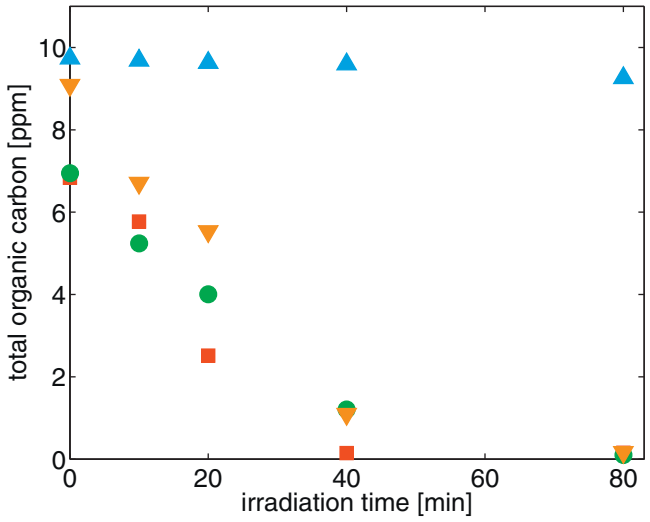

Fig. 4. Degradation of RBB determined by UV–vis spectrometry at 232 nm as a function of illumination time under full sunlight without any catalyst (▲), with 4% doped catalyst (▼), blank catalyst (●) and P25 (■).

adsorbed more RBB at lower pH values, it was oxidized equally quickly over the pH range studied. Therefore, all experiments were conducted at natural pH (5.1) of the dispersion (dye + C-doped TiO_2).

The catalysts dispersed in de-ionized water showed initial TOC values in the range of 2.5–3.5 ppm, a left over from the catalyst preparation procedure adsorbed to the surface. About half of this organic carbon was removed photocatalytically after 120 min illumination under full sunlight, as about 1.5 ppm carbon remained in solution.

Initial adsorption of the dye molecule (shown in Figs. 4 and 5 at time = 0) was much more pronounced for the un-doped catalysts (blank and P25) than for the doped ones. In these figures, only one doped catalyst is shown for clarity, as all the doped catalysts showed a very similar behavior in adsorption and photodegradation, except the sample labeled as 20% doped.

The doped catalysts were less efficient in adsorbing RBB compared to the un-doped catalysts, as can be observed by UV 232 nm measurement. The larger surface area of doped catalysts did not

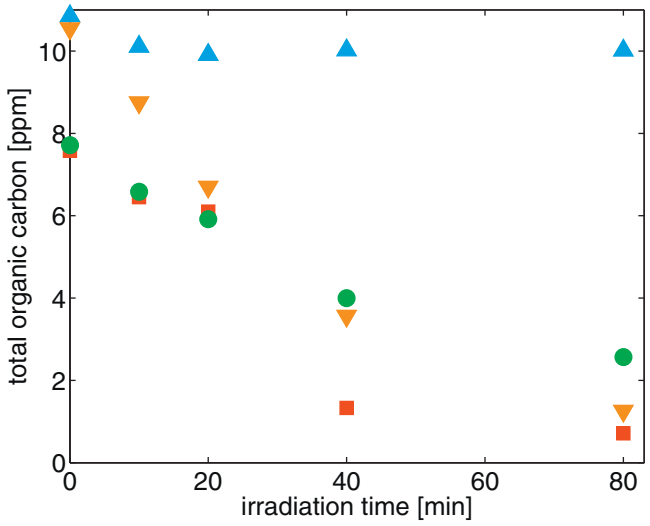

Fig. 5. Degradation of RBB determined by TOC as a function of illumination time under normal sunlight without any catalyst (▲), with blank catalyst (●), 4% doped catalyst (▼) and P25 (■).

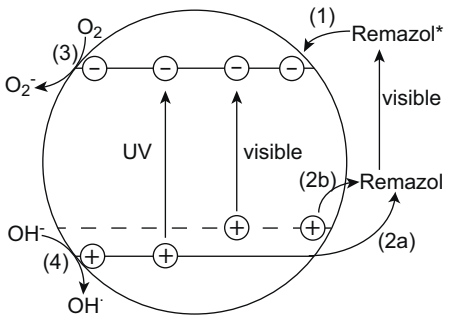

Fig. 6. Oxidation processes leading directly (1) and (2) or indirectly (3) and (4) to the degradation of RBB in the presence of doped TiO_2.

translate into increased adsorption but changes in surface structure due to C-doping or remaining carbon from the syntheses probably affected the RBB adsorption negatively.

3.5.1. Degradation under full sunlight

The dye was stable under illumination of full sunlight, as insignificant photo-degradation occurred in blank photo-reactions without catalyst (Figs. 4 and 5). All catalysts tested, except the 20% sample, efficiently degraded RBB under full sunlight. P25 was fastest in removing the initial molecule from solution; after 40 min of exposure, 98% RBB was removed, whereas the other catalysts removed around 90% in the same time. The total organic carbon removal was nearly complete (90%) within 80 min for all the catalysts except for the blank one. However, if the removal rate was analyzed, P25 and the doped catalysts had all very similar values (around 0.20 ppm/min) based on the UV analysis and slightly slower measured by the TOC analysis (around 0.18 ppm/min; as shown in Table 2). This indicates that the dye molecule is totally mineralized nearly at the same rate as the compound is initially oxidized. The observation that P25 and our doped catalysts revealed very similar degradation rates, suggests that under normal sunlight, the absorption of the UV part of the radiation causes the most efficient degradation of the dye molecules. Neither the increased surface area nor the increased absorption spectrum of our catalysts gave any enhanced efficiency compared to P25. In contrast, the same catalyst (4%) was less efficient than P25 to degrade 4-chlorophenol under full sunlight [37].

Two possible mechanisms can lead to the photo-degradation of the dye: Either the catalyst absorbs UV/visible light and reacts thereafter directly or indirectly with the dye or the dye absorbs UV/visible light and transfers an electron to the catalyst [49]. For two of these processes, the dye has to be in close contact with the catalyst (Fig. 6): (1) an excited dye injects an electron into the conduction band of the catalyst; (2) or the dye reacts directly with a hole located close to the catalysts surface. Finally, two further processes can lead to the dye degradation without a physical interaction of the dye and the catalyst: (3) two electrons react with oxygen to form H_2O_2 which can further react and yield hydroxyl radicals; or (4) a hole in the valence band reacts with a hydroxyl ion to generate also a hydroxyl radical. These hydroxyl radicals can then react with the dye and initiate its degradation. Under sunlight all these mechanisms are possible with RBB.

The interaction of negatively charged RBB with positively charged TiO_2 is probably relatively strong and was also reflected in the important initial adsorption. However, 4-chlorophenol, which has no charge and is much smaller, might not interact as strongly. Therefore, the two processes involving close contact of catalyst and pollutant (steps 1 and 2 in Fig. 6) were probably more important in the case of RBB than of 4-chlorophenol. One of the drawbacks of the C-doped catalysts may be the consumption of holes or electrons by color centers or localized states [22,40]. These mid-gap holes probably have poor mobility [45] and can only react with the pollutant (2b in Fig. 6) if the hole and also the pollutant are in close contact with the surface of the catalyst to compete with water oxidation [50]. However, these mid-gap holes are probably not capable to generate hydroxyl radicals [26,51]. Enhanced charge recombination would reduce the yield of not only route (4), but also (3) and (2a) and might explain the better performance with RBB than with 4-chlorophenol under sunlight of our catalysts compared to P25, due to more efficient processes (1) and (2) for RBB.

The fact that all catalysts had very similar degradation kinetics, even though their observed aggregated particle size determined by DLS varied greatly, indicates that aggregation of the TiO_2 particles had little or no impact on the degradation kinetics. The differences in aggregate size were not large enough to influence sufficiently their absorption coefficients and, hence, their photocatalytic activity [48]. Additionally, we evaluated as described elsewhere [52], that the extinction coefficient of P25 and the doped catalysts was too low that aggregates of the sizes reported here could efficiently shield light and reduce the light intensity at the core of the aggregates compared to the bulk phase.

The blank catalyst operated at reduced degradation rates, which can be attributed to lower light absorption and potentially reduced surface area as compared to the doped catalysts.

Surprisingly, the catalyst doped with 20% of melamine borate performed below expectations (Table 2), even though it showed better absorption of light in the visible wavelength region and had a BET surface area very similar to the other doped catalysts. The photo-degradation was therefore less efficient even though this catalyst absorbed more light and was equally efficient in adsorbing the dye molecules. A similar behavior was observed by Asahi et al. [19] for nitrogen doping, they argued that a change in crystal structure may have occurred due to high doping of nitrogen. From the XPS data we assumed that the carbon was not introduced

Table 2
Initial degradation rates determined by linear regression with 95% confidence intervals for experiments performed with and without 400 nm cut-off filter. UV analysis corresponds to the initial compound degradation, whereas TOC values represent total mineralization.

Sample	UV analysis: exp. without 400 nm cut-off filter (ppm/min)	TOC analysis: exp. without 400 nm cut-off filter (ppm/min)	UV analysis: exp. with 400 nm cut-off filter (ppm/min)	TOC analysis: exp. with 400 nm cut-off filter (ppm/min)
1%	0.199 ± 0.006	0.17 ± 0.03	0.025 ± 0.004	0.015 ± 0.005
2%	0.20 ± 0.05	0.17 ± 0.16	0.025 ± 0.002	0.020 ± 0.006
4%	0.20 ± 0.06	0.18 ± 0.03	0.023 ± 0.0014	0.013 ± 0.003
6%	0.21 ± 0.04	0.19 ± 0.02	0.023 ± 0.0012	0.011 ± 0.004
8%	0.20 ± 0.03	0.21 ± 0.07	0.023 ± 0.002	0.012 ± 0.003
12%	0.19 ± 0.04	0.17 ± 0.03	0.024 ± 0.002	0.013 ± 0.004
20%	0.15 ± 0.09	0.11 ± 0.03	0.019 ± 0.003	0.010 ± 0.004
P25	0.18 ± 0.11	0.16 ± 0.14	0.012 ± 0.003	−0.002 ± 0.003
Blank	0.14 ± 0.02	0.09 ± 0.02	0.013 ± 0.0014	0.006 ± 0.004
No catalyst	0.007 ± 0.0013	0.002 ± 0.010	0.0018 ± 0.0007	0.001 ± 0.006

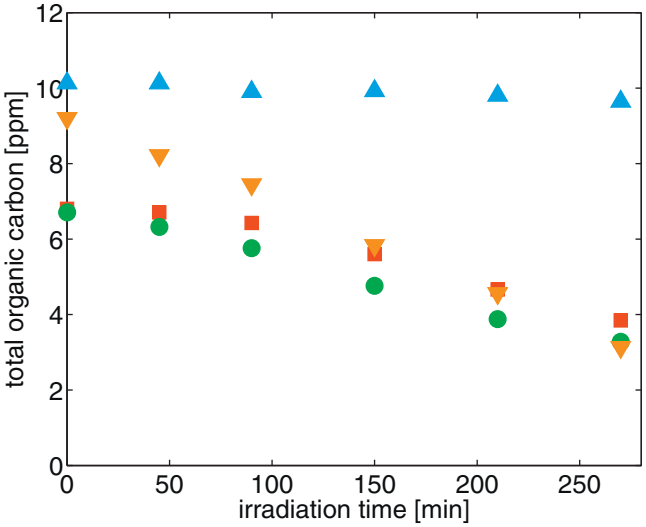

Fig. 7. Degradation of RBB determined by UV–vis spectrometry at 232 nm as a function of illumination time under cut-off sunlight (>400 nm) without any catalyst (▲), with blank catalyst (●), 4% doped catalyst (▼) and P25 (■).

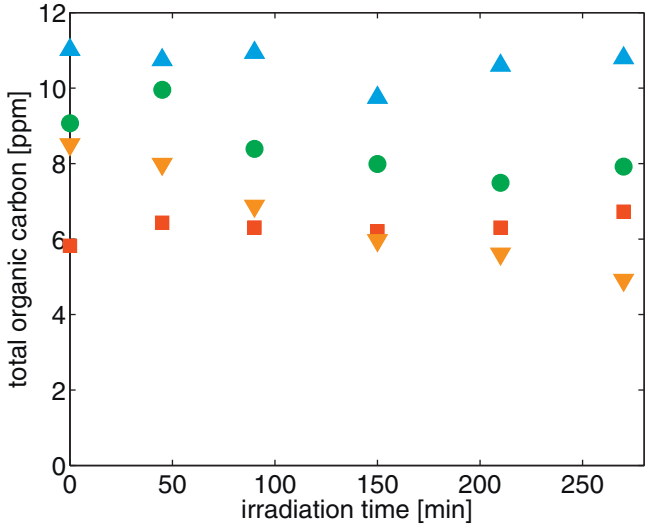

Fig. 8. Degradation of RBB determined by TOC as a function of illumination time under cut-off sunlight (>400 nm) without any catalyst (▲), with blank catalyst (●), 4% doped catalyst (▼) and P25 (■).

into the catalyst lattice as the binding energies did not increase for this catalyst compared to P25. The increased absorbance could be due to carbonaceous species on the catalyst surface, which did not improve the photocatalytic activity [46].

3.5.2. *Degradation with >400 nm cut-off filter*

The degradation rates were reduced about tenfold when light with shorter wavelengths than 400 nm was cut-off (Figs. 7 and 8 and Table 2). The efficiency of the photo-degradation process under visible light illumination was, therefore, much lower as only a small fraction of the total light falling under the absorption range as depicted in the absorption spectrum was now available for excitation. The holes created with wavelengths >400 nm are probably not energetic enough to generate hydroxyl radicals [26,51]. At the same time, the photo-generation of hydroxyl radicals from hydrogen peroxide is also stopped. H_2O_2 could accept another electron to generate a hydroxyl radical or trace metals (Fe or Cu) could generate hydroxyl radicals due to the Fenton process [53]. However, both processes consume more valence band electrons to generate hydroxyl radicals than the photo-generation from hydrogen peroxide, therefore reducing the overall yield. The reduction in efficiency under >400 nm indicates that under full sunlight, processes (4), (2a) and potentially (3) shown in Fig. 6 were the most effective to oxidize RBB, whereas (1) and (2b) were much less effective. Anthraquinone dyes are known to be bad electron donors from excited states [54], which agrees with a low yield due to (1). Another reason why the visible light induced states in the catalyst were much less effective is because they have poor mobility [45]. If they had been generated in the bulk of the catalyst aggregate, they would probably not been able to travel to the surface of the catalyst and react with RBB as is the case for excited states in the conduction or valence band (Fig. 6).

As for the experiments performed without using the cut-off filter, all doped catalysts excluding the 20% sample, showed very similar degradation rates around 0.024 ppm/min for the initial dye degradation. The values measured for the TOC removal were lower, ranging from 0.011 to 0.020 ppm/min. The confidence intervals were relatively high for these measurements due to the slow degradation kinetics and, therefore, the values, even though relatively varied, were not significantly different. The fact that several batches of catalysts showed very similar performances under both full sunlight and visible light clearly indicates that our synthesis method is very robust and reproducible.

Under visible light illumination only, the UV–vis spectral monitoring data showed about twice the initial rate than the TOC analysis for doped catalysts, which was not the case for full sunlight experiments. The catalysts had therefore, more difficulty to completely oxidize the organic compound under visible light alone compared to full UV + vis sunlight.

Different phenolic compounds were observed as intermediate products during RBB oxidation by P25 under UV irradiation due to hydroxyl radical attack [54]. Phenols are known to undergo decomposition under sunlight [55]. The partially oxidized dye products may therefore become more reactive and undergo photo-degradation. Under cut-off sunlight, the most energetic wavelengths were removed and the partially oxidized products may no longer absorb light that causes photo-degradation. Otherwise, under cut-off sunlight the photocatalyst probably produce no hydroxyl radicals, anymore. Hence, no easily oxidizeable products, such as phenols, were formed. As a result the downstream photochemistry and further mineralization of the degradation products was affected by the difference in the irradiation spectrum available under UV cut-off. In that case, the downstream products had to solely depend on the ability of the photocatalyst for further oxidation and mineralization. Finally, as the degradation kinetics were strongly reduced under UV cut-off sunlight, the absorbed species are more likely to desorb before they were completely mineralized. Therefore, the initial degradation of the organic compound was favored compared to the total mineralization, reducing the TOC compared to UV–vis values.

Even though P25 was able to remove some of the initial compound at about half the rate as the doped catalyst, it was, however, incapable of removing any organic carbon without UV radiation. P25 was probably capable of accepting electrons from the excited dye molecule (1) which might have led to discoloration [56]. However, it could not oxidize any of its carbon to CO_2. This clearly shows that carbon doping as proposed here with melanine borate allowed the catalysts to operate even under sunlight cut-off at 400 nm, which was not the case for conventional P25. Therefore, even if visible light photocatalysis (2b) is less efficient than UV processes, the localized holes generated have a sufficiently high oxidation potential to react with the electron-rich organic moieties of RBB, such as aniline or deprotonated amine [57] and can oxidize RBB nearly completely. Experiments performed over a longer period of time

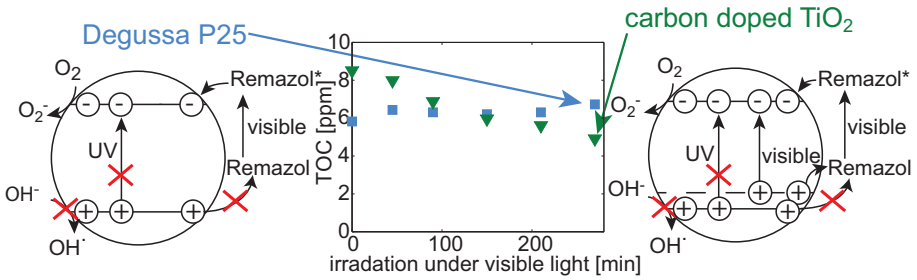

Fig. 9. Possible mechanisms degradation mechanisms for Degussa P25 and our carbon doped TiO_2 under visible light only.

showed that roughly 70% of the organic carbon was removed in 330 min.

In a parallel study [37], we showed that both the doped catalyst (4%) and P25 oxidized 4-chlorophenol even under cut-off sunlight but the doped catalyst was more efficient in reducing the TOC levels. P25 degrades 4-chlorophenol under visible light via a surface-complex mediated charge transfer [51], while RBB is a much larger and more stable molecule and was therefore more difficult to oxidize than 4-chlorophenol. Hence, our doped catalyst showed a clear advantage compared to P25 in degrading a stable dye molecule, as they could even operate under economical visible light. The initial breakdown of RBB to biodegradable fragments could easily be achieved with the doped catalyst and visible light alone. The final degradation could then be performed by biological decomposition.

As in the previous experiments, the catalysts doped with 20% had lower degradation rates compared to the other catalysts treated with lesser amounts of melamine borate (Table 2). The blank catalyst showed degradation although at roughly half the rate compared to the doped catalysts, which is in agreement with the small absorption in the visible light region.

4. Conclusions

This study reports the degradation kinetics of RBB by TiO_2 photocatalysts doped with melamine borate as reported in Neville et al. [37], compared to P25. Even though the initial dye adsorption was lower for the doped catalysts than for P25 the degradation rates of the dye were similar or faster under simulated sunlight for doped catalysts than for P25. The removal of any wavelength below 400 nm (removal of the UV fraction) stopped the total oxidation of the dye by P25, as the TOC value did not reduce during the experiment. However, the doped catalysts were still able, even though at a reduced rate, to remove 70% of the total organic carbon within 6.5 h. We suggest that mainly localized states above the valence band were capable of oxidizing the dye compound as shown in Fig. 9. Additionally, the blank catalyst showed degradation of the organic molecule under full sunlight and when a cut-off filter was employed. However, the rate was lower compared to doped catalysts from this study, indicating that doping definitely improved the catalysts performance. The percentage of carbon added in the form of melamine borate during the synthesis had no correlative effect on the catalyst morphology or its degradation kinetics. Only the 20 mol% melamine borate sample showed an increase in the light absorption pattern but reduced degradation kinetics of the dye.

Our doping method gave the catalysts the clear advantage to oxidize a large and stable molecule harvesting only cheap visible light and may therefore reduce the cost of treating wastewater from textile or printing industries, especially in combination with a post-biological treatment.

Acknowledgments

We thank César Pulgarin for providing us his TOC analyzer, Pascal Compte for performing the BET analysis, Nicolas Xanthopoulos for producing the XPS data, Guido Rothenberger for helping with the DRS measures and Adriana Paracchino for analyzing our samples with XRD.

References

[1] M.R. Hoffmann, S.T. Martin, W.Y. Choi, D.W. Bahnemann, Chemical Reviews 95 (1995) 69–96.
[2] D.F. Ollis, H. Al-Ekabi, Photocatalytic Purification and Treatment of Water and Air: Proceedings of the 1st International Conference on TiO_2 Photocatalytic Purification and Treatment of Water and Air, London/Ontario, Canada, 8–13 November, 1992, Elsevier, Amsterdam, New York, 1993.
[3] C.A. Grimes, O.K. Varghese, S. Ranjan, Light, Water, Hydrogen: The Solar Generation of Hydrogen by Water Photoelectrolysis, Springer, New York, 2008.
[4] M. Ni, M.K.H. Leung, D.Y.C. Leung, K. Sumathy, Renewable and Sustainable Energy Reviews 11 (2007) 401–425.
[5] J.L. Gole, J.D. Stout, C. Burda, Y.B. Lou, X.B. Chen, Journal of Physical Chemistry B 108 (2004) 1230–1240.
[6] A. Fujishima, X. Zhang, D.A. Tryk, Surface Science Reports 63 (2008) 515–582.
[7] M.A. Henderson, Surface Science Reports 66 (2011) 185–297.
[8] S. Rehman, R. Ullah, A.M. Butt, N.D. Gohar, Journal of Hazardous Materials 170 (2009) 560–569.
[9] A. Zaleska, Recent Patents on Engineering 2 (2008) 157–164.
[10] J.M. Herrmann, M.N. Mozzanega, P. Pichat, Journal of Photochemistry 22 (1983) 333–343.
[11] N. Serpone, D. Lawless, J. Disdier, J.M. Herrmann, Langmuir 10 (1994) 643–652.
[12] K. Lee, N.H. Lee, S.H. Shin, H.G. Lee, S.J. Kim, Materials Science and Engineering 129 (2006) 109–115.
[13] I. Nakamura, N. Negishi, S. Kutsuna, T. Ihara, S. Sugihara, E. Takeuchi, Journal of Molecular Catalysis A: Chemical 161 (2000) 205–212.
[14] I. Justicia, P. Ordejon, G. Canto, J.L. Mozos, J. Fraxedas, G.A. Battiston, R. Gerbasi, A. Figueras, Advanced Materials 14 (2002) 1399–1402.
[15] A.K. Ghosh, H.P. Maruska, Journal of the Electrochemical Society 124 (1977) 1516–1522.
[16] W.Y. Choi, A. Termin, M.R. Hoffmann, Journal of Physical Chemistry 98 (1994) 13669–13679.
[17] J.M. Herrmann, J. Disdier, P. Pichat, Chemical Physics Letters 108 (1984) 618–622.
[18] M. Anpo, Pure and Applied Chemistry 72 (2000) 1787–1792.
[19] R. Asahi, T. Morikawa, T. Ohwaki, K. Aoki, Y. Taga, Science 293 (2001) 269–271.
[20] S.U.M. Khan, M. Al-Shahry, W.B. Ingler, Science 297 (2002) 2243–2245.
[21] S. Sakthivel, H. Kisch, Angewandte Chemie-International Edition 42 (2003) 4908–4911.
[22] H. Irie, Y. Watanabe, K. Hashimoto, Journal of Physical Chemistry B 107 (2003) 5483–5486.
[23] T. Tachikawa, S. Tojo, K. Kawai, M. Endo, M. Fujitsuka, T. Ohno, K. Nishijima, Z. Miyamoto, T. Majima, Journal of Physical Chemistry B 108 (2004) 19299–19306.
[24] D. Chen, Z. Jiang, J. Geng, Q. Wang, D. Yang, Industrial and Engineering Chemistry Research 46 (2007) 2741–2746.
[25] X. Yang, C. Cao, K. Hohn, L. Erickson, R. Maghirang, D. Hamal, K. Klabunde, Journal of Catalysis 252 (2007) 296–302.
[26] Y. Park, W. Kim, H. Park, T. Tachikawa, T. Majima, W. Choi, Applied Catalysis B: Environmental 91 (2009) 355–361.
[27] F. Gähr, F. Hermanutz, W. Oppermann, Water Science and Technology 30 (1994) 255–263.
[28] F. Herrera, J. Kiwi, A. Lopez, V. Nadtochenko, Environmental Science and Technology 33 (1999) 3145–3151.
[29] E.J. Weber, V.C. Stickney, Water Research 27 (1993) 63–67.

[30] J.A. Ramsay, T. Nguyen, Biotechnology Letters 24 (2002) 1756–1760.
[31] C. Lizama, M.C. Yeber, J. Freer, J. Baeza, H.D. Mansilla, Water Science and Technology 44 (2001) 197–203.
[32] M. Siddique, R. Farooq, A. Shaheen, Journal of the Chemical Society of Pakistan 33 (2011) 284–293.
[33] D.C. Hurum, A.G. Agrios, K.A. Gray, T. Rajh, M.C. Thurnauer, Journal of Physical Chemistry B 107 (2003) 4545–4549.
[34] T. Ohno, K. Sarukawa, K. Tokieda, M. Matsumura, Journal of Catalysis 203 (2001) 82–86.
[35] A.K. Datye, G. Riegel, J.R. Bolton, M. Huang, M.R. Prairie, Journal of Solid State Chemistry 115 (1995) 236–239.
[36] D. Gumy, S.A. Giraldo, J. Rengifo, C. Pulgarin, Applied Catalysis B: Environmental 78 (2008) 19–29.
[37] E.M. Neville, M.J. Mattle, D. Loughrey, B. Rajesh, M. Rahman, J.M.D. MacElroy, J.A. Sullivan, K.R. Thampi, Journal of Physical Chemistry C 116 (2012) 16511–16521.
[38] G. Rothenberger, P. Comte, M. Gratzel, Solar Energy Materials and Solar Cells 58 (1999) 321–336.
[39] S.-I. In, A.H. Kean, A. Orlov, M.S. Tikhov, R.M. Lambert, Energy and Environmental Science 2 (2009) 1277.
[40] H. Irie, S. Washizuka, K. Hashimoto, Thin Solid Films 510 (2006) 21–25.
[41] H. Irie, Y. Watanabe, K. Hashimoto, Chemistry Letters 32 (2003) 772–773.
[42] S.-W. Hsu, T.-S. Yang, T.-K. Chen, M.-S. Wong, Thin Solid Films 515 (2007) 3521–3526.
[43] V.N. Kuznetsov, N. Serpone, Journal of Physical Chemistry B 110 (2006) 25203–25209.
[44] N. Serpone, Journal of Physical Chemistry B 110 (2006) 24287–24293.
[45] H. Wang, J.P. Lewis, Journal of Physics: Condensed Matter 18 (2006) 421–434.
[46] C. Xu, R. Killmeyer, M.L. Gray, S.U.M. Khan, Applied Catalysis B: Environmental 64 (2006) 312–317.
[47] A.L. Patterson, Physical Review 56 (1939) 978–982.
[48] T.A. Egerton, I.R. Tooley, Journal of Physical Chemistry B 108 (2004) 5066–5072.
[49] G.M. Liu, X.Z. Li, J.C. Zhao, H. Hidaka, N. Serpone, Environmental Science and Technology 34 (2000) 3982–3990.
[50] H. Liu, A. Imanishi, Y. Nakato, Journal of Physical Chemistry C 111 (2007) 8603–8610.
[51] S. Kim, W. Choi, Journal of Physical Chemistry B 109 (2005) 5143–5149.
[52] M.J. Mattle, T. Kohn, Environmental Science and Technology 46 (2012) 10022–10030.
[53] J.I. Nieto-Juarez, K. Pierzchła, A. Sienkiewicz, T. Kohn, Environmental Science and Technology 44 (2010) 3351–3356.
[54] M. Saquib, M. Muneer, Dyes Pigments 53 (2002) 237–249.
[55] A.L. Boreen, W.A. Arnold, K. McNeill, Aquatic Sciences 65 (2003) 320–341.
[56] W. Ren, Z. Ai, F. Jia, L. Zhang, X. Fan, Z. Zou, Applied Catalysis B: Environmental 69 (2007) 138–144.
[57] Y. Lee, U. von Gunten, Water Research 44 (2010) 555–566.